J Mater Sci: Mater Med (2009) 20:1223–1227
DOI 10.1007/s10856-008-3685-x

Synthesis of high purity hydroxyapatite nanopowder via sol–gel combustion process

Jiwen Wang · Leon L. Shaw

Received: 27 August 2008 / Accepted: 29 December 2008 / Published online: 10 January 2009

Abstract A polymeric sol–gel combustion method has been used to synthesize nanocrystalline hydroxyapatite (HA) powder from calcium nitrate and triethyl phosphate with the addition of NH_4OH. The sol–gel combustion process generates phase-pure nanocrystalline HA powder, as characterized using Fourier transform infrared (FTIR), X-ray diffraction (XRD), and transmission electron microscopy (TEM). Sintering of the HA powder compact at 1200°C for 2 h leads to a 93% theoretical dense ceramic body. This method offers an easy route for the preparation of phase-pure nanocrystalline HA powder.

1 Introduction

Hydroxyapatite ($Ca_{10}(PO_4)_6(OH)_2$, HA) is chemically similar to the mineral component of bones and hard tissues in mammals. It is bioactive, in that it supports bone ingrowth and osseointegration when used in orthopaedic, dental and maxillofacial applications. Hydroxyapatite powders can be synthesized via numerous production routes, using a range of different reactants. The main processing techniques include wet chemical methods (precipitation) [1–4], hydrothermal techniques [5–7] and sol–gel methods [8–12]. Although precipitation and hydrothermal methods are the most widely used approaches for synthesizing hydroxyapatite powders, the sol–gel method has its advantages over the others due to its simplicity, fast speed, homogeneous composition, and low synthesis temperature [9, 10]. However, reports on sol–gel derived HA powders indicate that synthesis of HA is frequently accompanied by secondary phases, such as calcium oxide (CaO), calcium carbonate ($CaCO_3$), and tricalcium phosphate (TCP) [10, 12, 13]. This is due to the incomplete gelation process, during which [–Ca–O–P–] oligomers are formed. Impure hydroxyapatite will cause decomposition in body fluid [14], and thus there is a need to produce phase-pure HA nanopowder by sol–gel method for a better bio-stability and bio-compatibility.

Kim et al. [13] have investigated the effect of adding NH_4OH to an ethanol–water-based hydroxyapatite sol–gel solution, and found that NH_4OH can enhance the gelation process to form pure HA coatings free from CaO, $CaCO_3$ and TCP. In this paper, we have examined the feasibility of synthesizing phase-pure HA nanopowder with the addition of NH_4OH in a sol–gel solution, followed by a subsequent combustion process. It is shown that the sol–gel combustion process using precursors of calcium nitrate and triethyl phosphite (TEP) with the addition of 5 vol % NH_4OH can produce phase-pure nanocrystalline HA powder. The as-synthesized powder exhibits good sinterability.

2 Experimental

The Ca solution was prepared by dissolving 2 M of calcium nitrate ($Ca(NO_3)_2 \cdot 4H_2O$, Sigma–Aldrich Company) in 100 ml ethanol at ambient temperature with stirring for 24 h. The P solution was prepared by hydrolyzing a stoichiometric amount (Ca/P = 1.67) of triethyl phosphite (TEP, Sigma–Aldrich Company) in an ethanol–water mixed solution (at a ratio of 6:1) with stirring for 24 h at room temperature. The Ca and P solutions were then mixed

J. Wang · L. L. Shaw (✉)
Department of Chemical, Materials and Biomolecular Engineering, Institute of Materials Science, University of Connecticut, Storrs, CT 06269, USA
e-mail: leon.shaw@uconn.edu

and stirred for 30 min at room temperature before adding 5% NH_4OH to the mixed solution. After the addition of NH_4OH the solution was stirred for an additional 30 min. Thereafter the solution was aged at 25°C for 20 h and then the aging temperature was increased to 50°C with additional holding at this new temperature for 55 h. The pH value of the HA solution was measured during the entire aging process. After aging, the solution was dried in an oven at 80°C for 12 h, which led to the formation of the HA gel. The dried HA gels were then put in a tube furnace and heated at 30°C/min to 350°C for 1 h to form HA nanopowder via a combustion process.

Dried HA gels were characterized using differential scanning calorimetry (DSC) and thermalgravimetric analysis (TGA) (SDT Q-600, New Castle, DE) to study the combustion process under an air flux (100 ml/min). Fourier transform infrared (FTIR, Nicolet Magna 560 FTIR spectrometers, Madison, WI), X-ray diffraction (XRD, Bruker D8 Advance X-Ray Diffractometers, Madison, WI), and transmission electron microscopy (TEM, JEOL 2010 FasTEM, Tokyo, Japan) were used to investigate the chemical state, phase composition, particle size and morphology of the HA gels and nanopowders. In addition to monitoring phase transformations, XRD was also used to estimate crystallite sizes of HA powder through the Scherrer formula [15]. The XRD peak broadening was attributed to the refinement of crystals and the instrumental effect. The correction for instrumental broadening was carried out using the procedure described in Ref. [16] with the aid of a coarse-grained Si as the standard. The specific surface area of HA nano powder was determined using a gas sorption analyzer (NOVE 1000 Surface Area Analyzer) based on the Brunauer–Emmett–Teller (BET) method [17].

To examine the sinterability, the combustion-formed HA nanopowder was calcined at 800°C for 2 h and then compressed into a disk with 1.27 mm diameter and 2 mm thickness, using a uniaxial pressing machine under a pressure of 340 MPa. Sintering of the disk was conducted at 1200°C for 2 h in a CM high temperature furnace (Bloomfield, NJ). The microstructure of the sintered HA body was observed using an environmental scanning electron microscope (ESEM, Philips ESEM 2020, Eindhoven, Netherlands).

3 Results and discussion

It is found that the pH value of the HA sol containing 5% NH_4OH changes with the aging time. As shown in Fig. 1, the initial pH value of the HA sol is 8.0 which decreases continuously with the aging time. Furthermore, the decrease rate in the pH value at 25°C is slower than that at 50°C. The decrease in the pH value is due to the increase of the H^+ concentration in the solution, indicating the progress of

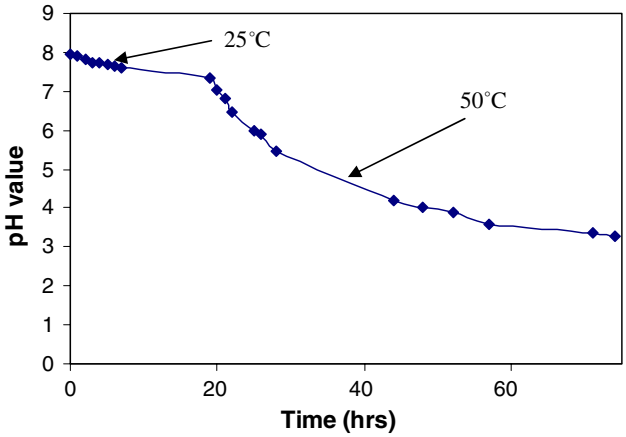

Fig. 1 The pH value of the HA sol with 5 vol % NH_4OH as a function of the aging time

dehydration and polymerization of the HA sol to form the HA gel. A simplified chemical formula [13] has been proposed to explain the increase of the H^+ concentration during the gelation process in which the Ca^+ ions react with the P–O single bond of the HO–P to form [–Ca–O–P–] oligomers and provide H^+ ions to the solution. The higher gelation rate observed at 50°C is consistent with the previous study [12] which reveals the strong temperature-dependent endothermic nature of the gelation due to the high activation energy of the gelation process. The addition of 5% NH_4OH provides a large number of OH^- ions to capture H^+ ions in the solution, thereby accelerating the gelation process [13]. Without the addition of NH_4OH, prolonged aging (up to 7 days) could be necessary in order to complete the gelation process to form HA with little secondary phases [12].

Figure 2 shows the simultaneous TGA and DSC curves of dried HA gels subjected to continuous heating to 1000°C

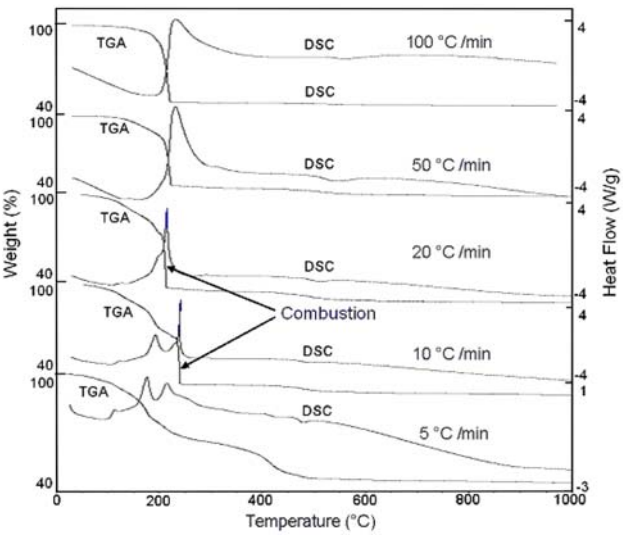

Fig. 2 DSC/TGA analysis of HA gels with different heating rates

with different heating rates. The total weight loss for all the samples is about 55% during the entire heating process. However, the decomposition behavior of HA gels changes with the heating rate. Specifically, at the heating rate of 5°C/min HA gels decomposed gradually from 25 to 500°C, accompanied by two sharp exothermic peaks near 200°C. There is almost no additional weight loss as well as no energy release/uptake above 500°C, indicating a stable phase thereafter. When the heating rate is increased to 10°C/min, a combustion process happens at 240°C with a sudden weight loss of about 47%, accompanied by a large amount of heat release. Additional heating above 240–600°C induces another 8% weight loss which is considered to be a completion of the decomposition of residual gels and the release of gases and bonded liquids. Above 600°C, no additional weight loss and energy release/uptake are observed. Further increases in the heating rate to 20°C/min or higher reduce the combustion temperature down to 200°C and the two exothermic peaks merge into one. Such a phenomenon is attributed to the high accumulation of the decomposition energy owing to the higher heating rates. It is noted that the combustion temperature is highly sensitive to the aging time of dried gels (not shown here). A longer aging time and lower concentration of the volatile solvent in the HA gel will result in a higher combustion temperature.

Figure 3 shows FTIR spectra of HA gels formed at 50°C with and without subsequent thermal exposure to 200, 300, 600, and 1000°C for 1 h with a heating rate of 10°C/min from the ambient to the defined temperature. The FTIR spectra of dried and 200°C treated HA gels show strong N–O band at 1400 cm^{-1}, which is from the crystalline nitrate. Furthermore, the characteristic bands from

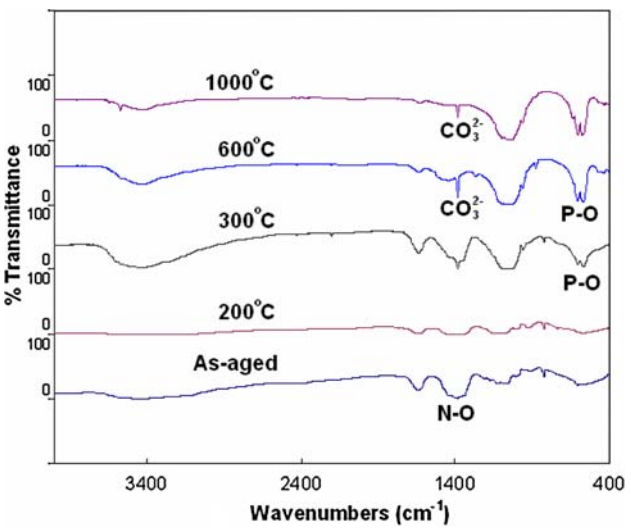

Fig. 3 FTIR spectra of HA gels after heating at different temperatures

~500 to 600 cm^{-1} and 1000 to 1100 cm^{-1} related to the vibrational modes of phosphate ions are very weak, indicating the presence of little apatite structure. However, the characteristic P–O bands (~500–600 and 1000–1100 cm^{-1}) become more definite and stronger after HA gel is treated at 300°C (above the combustion temperature), indicating the formation of the apatite phase by combustion process. These P–O bands become even more definite after HA is treated at 600°C and 1000°C, indicating that the apatite structure matures to a high degree with better crystallization. Accompanied with the development of P–O bands at 300°C or higher, the intensities of hydroxyl ions with the stretching vibration at 3570 cm^{-1} also become apparent and stronger, confirming the formation of HA. The presence of C–O bands at ~1420–1450 cm^{-1} associated with the vibrational modes of carbonate ions suggests the partial OH^- substitution by CO_3^{2-} in the combustion-formed HA powder.

The XRD pattern (Fig. 4) of the combustion-formed HA powder obtained by heating the HA gel at 350°C for 1 h with a heating rate of 30°C/min from ambient to 350°C shows characteristic peaks of pure hydroxyapatite phase. No second phases, such as CaO or TCP, are found. In contrast, the presence of CaO has been reported previously, in similar studies using sol–gel processes for making HA coatings and powders [10, 12]. The improved phase purity is mainly due to the addition of NH_4OH with proper aging time of the HA sol, during which Ca^{2+} ions completely react with the P–O single bond of the HO–P to form [–Ca–O–P–] chains—the backbone of crystalline HA. The OH^- ions provided by NH_4OH serve to neutralize the H^+ ions produced from the gelation reaction and thus accelerate the gelation process [13].

The grain size of the HA nanopowder, combustion formed and heat treated at 350°C for 1 h, determined by TEM (Fig. 5) is between 50 to 100 nm, which is in good

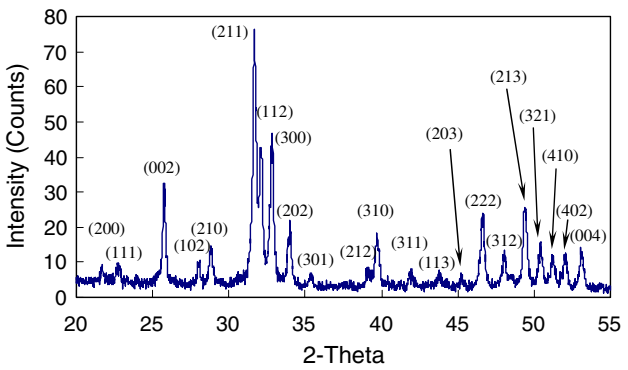

Fig. 4 XRD pattern of the HA powder synthesized after heating at 350°C for 1 h. All the major peaks from the crystalline HA have been labeled. Clearly, every single peak has been accounted for by the crystalline HA

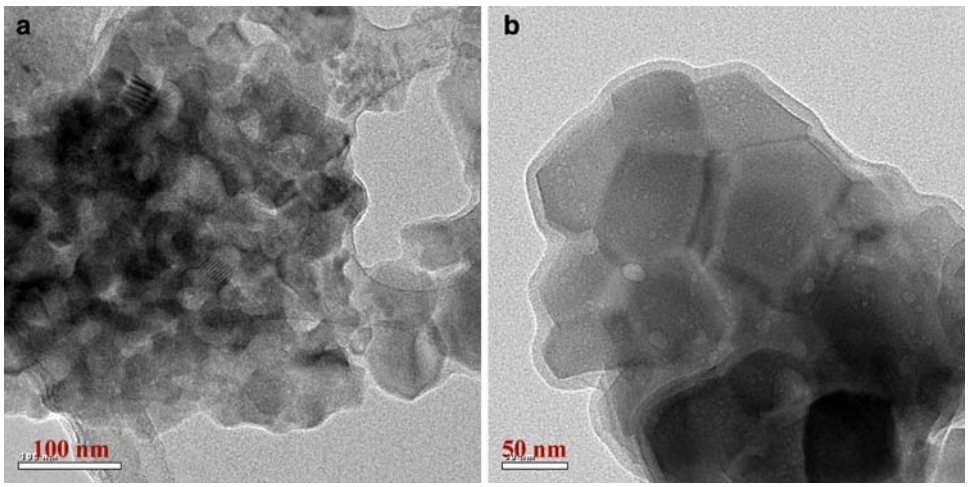

Fig. 5 TEM image of the as-synthesized HA nanopowder after heating at 350°C for 1 h: **a** a general view and **b** a closer view of the HA powder

accordance with the average crystallite size of 80 nm estimated from the peak broadening of (002) reflection of the XRD pattern using the Scherrer formula. The specific surface area of the nanopowder is found to be 13 m^2/g, which gives rise to an equivalent particle size of 150 nm assuming that all the particles are spherical. Comparing the grain size and the equivalent particle size reveals that the as-synthesized HA powder is nanocrystalline with slightly agglomeration.

After calcination of the HA nanopowder at 800°C for 2 h, the powder was compacted via uniaxial pressing with a pressure of 340 MPa and the powder compact was sintered at 1200°C in an air atmosphere for 2 h. After sintering, the hydroxyapatite ceramic body achieved a density of 93% of the theoretical value (3.16 g/cm^3). Microstructure analysis (Fig. 6) shows grain sizes ranging from 1 to 3 μm, with some uniformly dispersed micron pores.

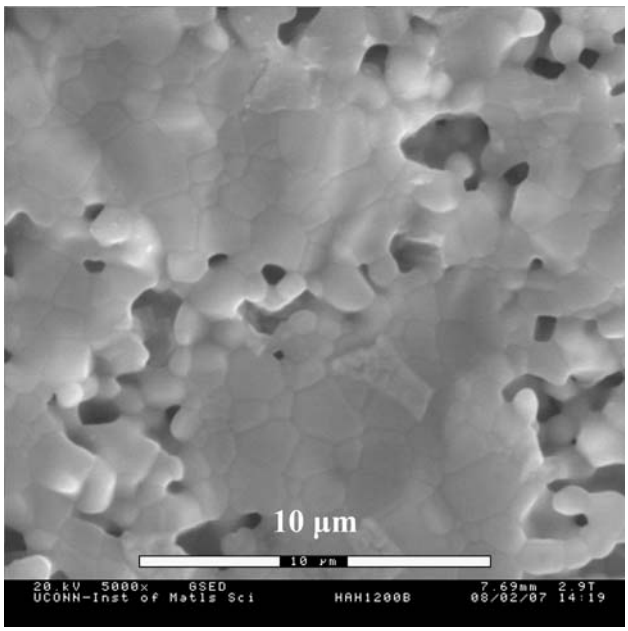

Fig. 6 SEM microstructure image of the 1200°C-sintered HA body

4 Conclusions

Phase-pure nanocrystalline hydroxyapatite powder was obtained by a sol–gel combustion process using precursors of calcium nitrate and TEP with the addition of 5 vol% NH_4OH. The combustion process happens at the temperature as low as 200°C with a heating rate higher than 20°C/min. The synthesized powder has grain sizes ranging from 50 to 100 nm with an average size of 80 nm. HA bodies sintered at 1200°C for 2 h have a relative density of 93%. This process provides a simple and fast way for making pure nanocrystalline hydroxyapatite powder.

References

1. M. Jarcho, C.H. Bolen, M.B. Thomas, J. Bobick, J.F. Kay, R.H. Doremus, Hydroxylapatite synthesis and characterization in dense polycrystalline form. J. Mater. Sci. **11**, 2027–2035 (1976). doi:10.1007/BF02403350
2. T. Ishikawa, H. Tanaka, A. Yasukawa, K. Kandori, Modification of calcium hydroxyapatite using ethyl phosphates. J. Mater. Chem. **5**, 1963–1967 (1995). doi:10.1039/jm9950501963
3. K. Kandori, A. Yasukawa, T. Ishikawa, Preparation and characterization of spherical calcium hydroxyapatite. Chem. Mater. **7**, 26–32 (1995). doi:10.1021/cm00049a007
4. J. Wang, L. Shaw, Morphology-enhanced low-temperature sintering of nanocrystalline hydroxyapatite. Adv. Mater. **19**, 2364–2369 (2007). doi:10.1002/adma.200602333
5. T. Hattori, Y. Lwadate, Hydrothermal preparation of calcium hydroxyapatite powders. J. Am. Ceram. Soc. **73**, 1803–1805 (1990). doi:10.1111/j.1151-2916.1990.tb09841.x
6. J. Liu, X. Ye, H. Wang, M. Zhu, B. Wang, H. Yan, The influence of pH and temperature on the morphology of hydroxyapatite synthesized by hydrothermal method. Ceram. Int. **29**, 629–633 (2003). doi:10.1016/S0272-8842(02)00210-9

7. Y. Fujishiro, H. Yabuki, K. Kawamura, T. Sato, A. Okuwaki, Preparation of needle-like hydroxyapatite by homogeneous precipitation under hydrothermal conditions. J. Chem. Technol. Biotechnol. **57**(4), 349–353 (1993)
8. M.-F. Hsieh, L.-H. Perng, T.-S. Chin, H.-G. Perng, Phase purity of sol–gel-derived hydroxyapatite ceramic. Biomaterials **22**, 2601–2607 (2001). doi:10.1016/S0142-9612(00)00448-8
9. H.K. Varma, S.N. Kalkurab, R. Sivakumaf, Polymeric precursor route for the preparation of calcium phosphate compounds. Ceram. Int. **24**, 467–470 (1998). doi:10.1016/S0272-8842(97)00038-2
10. Y. Han, S. Li, X. Wang, X. Chen, Synthesis and sintering of nanocrystalline hydroxyapatite powders by citric acid sol–gel combustion method. Mater. Res. Bull. **39**, 25–32 (2004). doi:10.1016/j.materresbull.2003.09.022
11. W. Weng, J.L. Baptista, Synthesis of calcium phosphates by $PO(OH)_x(OBut)_{3-x}$ and $CaO_2C_2H_4$. J. Sol–Gel. Sci. Technol. (Paris) **8**, 645–649 (1997)
12. D.-M. Liu, T. Troczynski, W.J. Tseng, Aging effect on the phase evolution of water-based sol–gel hydroxyapatite. Biomaterials **23**, 1227–1236 (2002). doi:10.1016/S0142-9612(01)00242-3
13. H.-W. Kim, H.-E. Kim, J.C. Knowles, Improvement of hydroxyapatite sol–gel coating on titanium with ammonium hydroxide addition. J. Am. Ceram. Soc. **88**, 154–159 (2005)
14. Y. Li, W. Weng, K.C. Tam, Novel highly biodegradable biphasic tricalcium phosphates composed of α-tricalcium phosphate and β-tricalcium phosphate. Acta Biomater. **3**, 251–254 (2007). doi:10.1016/j.actbio.2006.07.003
15. H.P. Klug, L.E. Alexander, *X-ray diffraction procedures for polycrystalline and amorphous materials* (Wiley, London, 1954)
16. L. Shaw, J. Villegas, H. Luo, D. Miracle, Thermal stability of nanostructured $Al_{93}Fe_3Ti_2Cr_2$ alloys prepared via mechanical alloying. Acta Mater. **51**, 2647–2663 (2003). doi:10.1016/S1359-6454(03)00075-2
17. S. Brunauer, P.H. Emmett, E. Teller, Adsorption of gases in multimolecular layers. J. Am. Chem. Soc. **60**, 309–319 (1938). doi:10.1021/ja01269a023